JOURNAL OF THE KOREAN ASTRONOMICAL SOCIETY
34: S215 ~ S224, 2001

Numerical Method for General Relativistic Magnetohydrodynamics in Kerr Space-Time

SHINJI KOIDE
Department of Engineering, Toyama University, 3190 Gofuku, Toyama 930-8555, Japan
E-mail: koidesin@ecs.toyama-u.ac.jp

KAZUNARI SHIBATA
Kwasan and Hida Observatory, Kyoto University, Yamashina, Kyoto 607-8471, Japan
E-mail: shibata@kwasan.kyoto-u.ac.jp

TAKAHIRO KUDOH
National Astronomical Observatory, Mitaka, Tokyo 181-8588, Japan
E-mail: kudoh.takahiro@nao.ac.jp

AND DAVID L. MEIER
Jet Propulsion Laboratory, 4800 Oak Grove Drive, Pasadena, CA 91109, USA
E-mail: dlm@sgra.jpl.nasa.gov

(Received Oct. 31, 2001; Accepted Nov. 15, 2001)

ABSTRACT

We present the whole basis of numerical method and useful formulae for general relativistic magnetohydrodynamic simulations in Kerr space-time.

Key Words : general relativity, magnetohydrodynamics, Kerr black hole, numerical method

I. INTRODUCTION

Relativistic jets now have been discovered in several different classes of objects, including active galactic nuclei (Pearson & Zensus 1987; Biretta, Sparks, & Macchetto 1999), micro-quasars (Mirabel & Rodriguez 1994; Tingay et al. 1995), and gamma-ray bursts (Kulkarni et al. 1999). It is believed that a rapidly spinning black hole exists at the center of each of these objects and that the violent phenomena that occur near the hole is responsible for the jets. Dynamics of magnetized plasma around Kerr black hole is one of the most promising candidates of the process in the violent phenomena. In order to understand the basic physics of dynamics of magnetized plasma around a black hole, we have developed a numerical method for general relativistic magnetohydrodynamic (GRMHD) simulations in Kerr space-time (Koide, Meier, Shibata, & Kudoh 2000). In this paper, we present the whole basic method for it (Sections II and III) and summarize the useful formulae for the test problems of the GRMHD code (Section IV). An example of the GRMHD simulation is shown in Section V.

II. BASIC EQUATIONS

(a) Four-dimensional Form of GRMHD Equations

In order to understand the basic physics of plasmas around a black hole, numerical method of general relativistic MHD is demanded. The method is based on the general relativistic formulation of the laws of particle number, energy-momentum, Maxwell equations, and Ohm's law with zero electrical resistance (*ideal MHD condition*) on curved space-time (Weinberg 1972; Koide, Shibata, & Kudoh 1999; Koide et al. 2000). The space-time $(x^0, x^1, x^2, x^3) = (ct, x^1, x^2, x^3)$ is described by metric $g_{\mu\nu}$, where the line element ds is given by $(ds)^2 = g_{\mu\nu}dx^\mu dx^\nu$. Here, c is the speed of light. The basic equations of GRMHD in four-dimensional space-time are

$$\nabla_\nu(\rho U^\nu) = \frac{1}{\sqrt{-||g||}}\frac{\partial}{\partial x^\nu}(\sqrt{-||g||}\rho U^\nu) = 0, \quad (1)$$

$$\nabla_\nu T^{\mu\nu} = \frac{1}{\sqrt{-||g||}}\frac{\partial}{\partial x^\nu}(\sqrt{-||g||}T^{\mu\nu}) + \Gamma^\mu_{\sigma\nu}T^{\sigma\nu} = 0, \quad (2)$$

$$\partial_\mu F_{\nu\lambda} + \partial_\nu F_{\lambda\mu} + \partial_\lambda F_{\mu\nu} = 0, \quad (3)$$

$$\nabla_\mu F^{\mu\nu} = -\mu_0 J^\nu, \quad (4)$$

where ∇_ν is covariant derivative; $||g||$ is the determinant of the matrix with the element $g_{\mu\nu}$; $\Gamma^\lambda_{\mu\nu} \equiv \frac{1}{2}g^{\lambda\sigma}\left(-\frac{\partial g_{\mu\nu}}{\partial x^\sigma} + \frac{\partial g_{\nu\sigma}}{\partial x^\mu} + \frac{\partial g_{\sigma\mu}}{\partial x^\nu}\right)$ is Christoffel symbol. Here, U^ν and $J^\nu = (c\rho_e, J^1, J^2, J^3)$ are four-velocity and four-current density, respectively (ρ_e is the electric charge density); the general relativistic energy momentum tensor $T^{\mu\nu}$ is given by

$$T^{\mu\nu} = pg^{\mu\nu} + (e_{\rm int} + p)U^\mu U^\nu + F^\mu_\sigma F^{\nu\sigma} - \frac{1}{4}g^{\mu\nu}F^{\lambda\kappa}F_{\lambda\kappa}, \quad (5)$$

where $F^{\mu\nu}$ is the electromagnetic field-strength tensor, $F_{\mu\nu} = \partial_\mu A_\nu - \partial_\nu A_\mu$ and $A^\mu = (\phi_e/c, A^1, A^2, A^3)$ is

four-vector potential (ϕ_e is the electro-static potential). The electric field E_i and the magnetic field B_i are given by $E_i = cF_{i0}$ $(i = 1, 2, 3)$ and $B_1 = F_{23}$, $B_2 = F_{31}$, $B_3 = F_{12}$, respectively. Scalar values ρ, p, and $e_{\rm int}$ are proper mass density, proper pressure, and proper internal energy density $e_{\rm int} = \rho c^2 + p/(\Gamma - 1)$, respectively, where Γ is the specific heat ratio. In equation (4), μ_0 is the magnetic permeability in the vacuum. In addition to the equations, we assume the infinite electric conductivity condition

$$F_{\mu\nu}U^\nu = 0. \tag{6}$$

Using this condition, equations (1)-(3) close self-consistently. Equation (4) is used only to calculate the current density J^μ.

We assume that the off-diagonal spatial elements of the metric $g_{\mu\nu}$ vanish,

$$g_{ij} = 0 \quad (i \neq j). \tag{7}$$

Here Roman number (i,j) runs from 1 to 3, while Greek number (μ, ν, λ) runs from 0 to 3. We write

$$g_{00} = -h_0^2, \quad g_{ii} = h_i^2, \tag{8}$$

$$g_{i0} = g_{0i} = -h_i^2\omega_i/c. \tag{9}$$

Then the scale of small element in the space-time is given by

$$(ds)^2 = g_{\mu\nu}dx^\mu dx^\nu = -h_0^2(cdt)^2 + \sum_{i=1}^{3}[h_i^2(dx^i)^2 - 2h_i^2\omega_i dt dx^i] \tag{10}$$

When we define the lapse function α and 'shift velocity' (shift vector) β^i as

$$\alpha = \sqrt{h_0^2 + \sum_{i=1}^{3}\left(\frac{h_i\omega_i}{c}\right)^2}, \tag{11}$$

$$\beta^i = \frac{h_i\omega_i}{c\alpha}, \tag{12}$$

the line element ds is written as

$$(ds)^2 = -\alpha^2(cdt)^2 + \sum_{i=1}^{3}(h_i dx^i - c\beta^i\alpha dt)^2. \tag{13}$$

Furthermore, the contravariant metric is written explicitly as

$$g^{00} = -\frac{1}{\alpha^2}, \tag{14}$$

$$g^{i0} = g^{0i} = -\frac{1}{\alpha^2}\frac{\omega_i}{c} \tag{15}$$

$$g^{ij} = \frac{1}{h_i h_j}(\delta^{ij} - \beta^i\beta^j). \tag{16}$$

(b) Kerr Space-time

A Kerr black hole has two characteristic parameters, the mass M and the angular momentum J. We often use the rotation parameter $a = J/J_{\rm max}$, where $J_{\rm max} = GM^2/c$ is the angular momentum of the maximumly rotating black hole with the mass M ($G = 6.67 \times 10^{-11}{\rm Nm^2/kg^2}$ is the gravitational constant). In the Boyer-Lindquist frame $(x^0, x^1, x^2, x^3) = (ct, r, \theta, \phi)$, the metric of Kerr space-time is written as,

$$h_0 = \sqrt{1 - \frac{2r_g r}{\Sigma}}, h_1 = \sqrt{\frac{\Sigma}{\Delta}}, h_2 = \sqrt{\Sigma}, h_3 = \sqrt{\frac{A}{\Sigma}}\sin\theta, \tag{17}$$

$$\omega_1 = \omega_2 = 0, \quad \omega_3 = \frac{2cr_g^2 ar}{A}, \tag{18}$$

where $r_g \equiv GM/c^2$ is called the gravitational radius, $\Delta = r^2 - 2r_g r + (ar_g)^2$, $\Sigma = r^2 + (ar_g)^2\cos^2\theta$, and $A = \{r^2 + (ar_g)^2\}^2 - \Delta(ar_g)^2\sin^2\theta$. In this metric, the lapse function is $\alpha = \sqrt{\Delta\Sigma/A}$. The radius of the event horizon is $r_H = r_g(1 + \sqrt{1 - a^2})$, which comes from $\alpha = 0$. We also often use Schwarzschild radius of the black hole, $r_S = 2GM/c^2 = 2r_g$.

The rotating black hole drags the space around it. This is called *frame-dragging* effect. It causes the special region around it, in which any matter, energy and information should rotate in the same direction as the black hole rotation. This region is called *ergosphere*. The surface of the ergosphere is given by $h_0 = 0$, that is $r = r_g(1 + \sqrt{1 - a^2\cos^2\theta})$. In the ergosphere, the shift velocity $c\beta^\phi$ is greater than the light speed. The shape of the surface is like that of an apple in a high rotation parameter case ($a \sim 1$), with a cusp-like dimple at the top and bottom: at the pole it touches the horizon $r = r_H$ and on the equatorial plane, the radius is r_S. In the low rotation parameter case, $a < 0.8$, the shape is like an ellipsoid.

(c) 3+1 Formalism of GRMHD Equations

We present the 3+1 formalism of general relativistic MHD (GRMHD) equations derived from the four-dimensional expressions (1) - (4), and (6). We use several frames to observe physical quantities as follows.

- Laboratory frame
  This is a global frame fixed to the observer far from the black hole. In the astrophysics, it may be better that it is called 'Observer-at-infinity' frame. In the Kerr space-time, we refer the frame by Boyer-Lindquist (BL) frame. Here we write any contravariant vector by a^μ.

- Local laboratory (LOLA) frame
  There is no popular terminology for this frame, while it is useful. An observer on this frame *sees* events locally, that is, only the events at the

neighborhood. Furthermore, it is fixed to the laboratory frame. In the frame $(c\tilde{t}, \tilde{x}^1, \tilde{x}^2, \tilde{x}^3)$, the line element is written as

$$(ds)^2 = -(cd\tilde{t})^2 + \sum_i (d\tilde{x}^i - c\beta^i d\tilde{t})^2, \quad (19)$$

where $cd\tilde{t} = \alpha cdt$, $d\tilde{x}^i = h_i dx^i$. Therefore, the covariant vector measured by 'LOLA' frame is related with a^μ as

$$\tilde{a}^0 = \alpha a^0, \quad \tilde{a}^i = h_i a^i. \quad (20)$$

The covariant vector by 'LOLA' frame is

$$\tilde{a}_0 = \frac{1}{\alpha} a_0, \quad \tilde{a}_i = \frac{1}{h_i} a_i. \quad (21)$$

- Fiducial observer (FIDO) frame

  This is a locally inertial frame. Using the coordinates of the frame $(c\hat{t}, \hat{x}^1, \hat{x}^2, \hat{x}^3)$, the line element is

$$(ds)^2 = -(c\hat{dt})^2 + \sum_i (d\hat{x}^i)^2, \quad (22)$$

  where $c\hat{dt} = cd\tilde{t}$, $d\hat{x}^i = d\tilde{x}^i - \beta^i cd\tilde{t}$. This is the same as that of Minkovski space-time. The contravariant vector by 'FIDO' frame $\hat{a}^\mu$ is

$$\hat{a}^0 = \tilde{a}^0, \quad \hat{a}^i = \tilde{a}^i - \tilde{a}^0 \beta^i. \quad (23)$$

  With respect to covariant vector $\hat{a}_\mu$, we find

$$\hat{a}_0 = \tilde{a}_0 + \sum_i \beta^i \tilde{a}_i, \quad \hat{a}_i = \tilde{a}_i. \quad (24)$$

  It is noted that $\hat{a}^0 = -\hat{a}_0$ and $\hat{a}^i = \hat{a}_i$.

- Comoving frame

  Observer on this frame *rides on* the gas or the plasma to see events locally. The quantity observed by this frame is often called *proper* values because it is dependent only on the nature of the gas or plasma itself. Any scalar quantity is measured by this frame.

The components of vectors and tensors measured by 'LOLA' frame are given by equations (20), (21). To get transformation of any tensor like $q^{\mu\nu}$ we just consider the product of vectors like $a^\mu b^\nu$. Here, we denote these components with tilde. We find,

$$\tilde{\gamma} = \alpha U^0, \quad (25)$$

$$\tilde{v}^i = \frac{h_i}{\tilde{\gamma}} c U^i, \quad (26)$$

$$\tilde{T}^{00} = \alpha^2 T^{00}, \quad (27)$$

$$\tilde{P}^i = \frac{\alpha h_i}{c} T^{i0} = \frac{\alpha h_i}{c} T^{0i}, \quad (28)$$

$$\tilde{T}^{ij} = h_i h_j T^{ij}, \quad (29)$$

$$\tilde{F}_{0i} = -\tilde{F}_{i0} = \frac{1}{\alpha h_i} F_{0i}, \quad (30)$$

$$\tilde{F}_{ij} = -\tilde{F}_{ij} = \frac{1}{h_i h_j} F_{ij}, \quad (31)$$

$$\tilde{\rho}_{\rm e} = \frac{\tilde{J}^0}{c} = \frac{1}{c} \alpha^2 J^0, \quad (32)$$

$$\tilde{J}^i = \alpha h_i J^i. \quad (33)$$

Usually we use physical variables measured by FIDO, which are given by equations (23) and (24) as

$$\hat{\gamma} = \tilde{\gamma}, \quad (34)$$

$$D = \hat{\gamma}\rho, \quad (35)$$

$$\hat{v}^i = \tilde{v}^i - c\beta^i, \quad (36)$$

$$\epsilon + Dc^2 = \hat{T}^{00} = \tilde{T}^{00}, \quad (37)$$

$$\hat{P}^i = \tilde{P}^i - \frac{1}{c}\beta^i \tilde{T}^{00} = \tilde{P}^i - \frac{\beta^i}{c}(\epsilon + Dc^2), \quad (38)$$

$$\hat{T}^{ij} = \tilde{T}^{ij} - \beta^i \tilde{T}^{0j} - \beta^j \tilde{T}^{i0} + \beta^i \beta^j \tilde{T}^{00}, \quad (39)$$

$$\hat{F}_{i0} = -\hat{F}_{0i} = \tilde{F}_{0i} + \sum_j \beta^j \tilde{F}_{ij}, \quad (40)$$

$$\hat{F}_{ij} = \tilde{F}_{ij}, \quad (41)$$

$$\hat{\rho}_{\rm e} = \tilde{\rho}_{\rm e}, \quad (42)$$

$$\hat{J}^i = \tilde{J}^i - \hat{\rho}_{\rm e} c\beta^i, \quad (43)$$

where $\hat{\gamma}$ is Lorentz factor; $\hat{v}^i$ is three-velocity; ϵ is energy density; and $\hat{P}^i$ is momentum density. We usually write as $\gamma = \hat{\gamma}$ and $\rho_{\rm e} = \hat{\rho}_{\rm e}$.

The relationship between the variables measured by FIDO is the same as that of special relativistic MHD. Here, we summarize the relation.

$$D = \gamma\rho, \quad (44)$$

$$\gamma = \frac{1}{\sqrt{1 - \sum_{i=1}^3 (\hat{v}^i/c)^2}}, \quad (45)$$

$$\hat{P}^i = \frac{1}{c^2} h\gamma^2 \hat{v}^i + \frac{1}{c^2}(\hat{\mathbf{E}} \times \hat{\mathbf{B}})_i, \quad (46)$$

$$\hat{T}^{ij} = p\delta^{ij} + \frac{h}{c^2}\gamma^2 \hat{v}^i \hat{v}^j + \left(\frac{\hat{B}^2}{2} + \frac{\hat{E}^2}{2c^2}\right)\delta^{ij} - \hat{B}^i \hat{B}^j - \frac{\hat{E}^i \hat{E}^j}{c^2}, \quad (47)$$

$$\epsilon = h\gamma^2 - p - Dc^2 + \frac{\hat{B}^2}{2} + \frac{\hat{E}^2}{2c^2}, \quad (48)$$

where h is the relativistic enthalpy density, $h = \rho c^2 + \Gamma p/(\Gamma - 1) = e_{\rm int} + p$. Here, the magnetic $\hat{\mathbf{B}}$ and the electric field $\hat{\mathbf{E}}$ are defined as

$$\hat{B}_i = \sum_{j,k} \frac{1}{2} \epsilon^{ijk} \hat{F}_{jk}, \quad (49)$$

$$\hat{E}_i = c\hat{F}_{i0}. \tag{50}$$

There is relation as follows,

$$\hat{B}_i = \tilde{B}_i, \tag{51}$$

$$\hat{E}_i = \tilde{E}_i + \sum_{j,k} \epsilon^{ijk} c\beta^j \tilde{B}_k, \tag{52}$$

where

$$\tilde{B}_i = \sum_{j,k} \frac{1}{2}\epsilon^{ijk}\tilde{F}_{jk}, \tag{53}$$

$$\tilde{E}_i = c\tilde{F}_{i0}. \tag{54}$$

Using the FIDO variables, we derive the following set of equations from the general relativistic conservation laws of plasma and Maxwell equations (1)-(4) and (6).

$$\frac{\partial D}{\partial t} = -\frac{1}{h_1h_2h_3}\sum_i \frac{\partial}{\partial x^i}\left[\frac{\alpha h_1h_2h_3}{h_i} D(\hat{v}^i + c\beta^i)\right], \tag{55}$$

$$\frac{\partial \hat{P}^i}{\partial t} = -\frac{1}{h_1h_2h_3}\sum_j \frac{\partial}{\partial x^j}\left[\frac{\alpha h_1h_2h_3}{h_j}(\hat{T}^{ij} + c\beta^j\hat{P}^i)\right] - (\epsilon + Dc^2)\frac{1}{h_i}\frac{\partial \alpha}{\partial x^i} + \alpha f^i_{\rm curv} - \sum_j \hat{P}^j\sigma_{ji}, \tag{56}$$

$$\frac{\partial \epsilon}{\partial t} = -\frac{1}{h_1h_2h_3}\sum_i \frac{\partial}{\partial x^i}\left[\frac{\alpha h_1h_2h_3}{h_i} c^2(\hat{P}^i - D\hat{v}^i + \frac{\beta^i}{c}\epsilon)\right] - \sum_i c^2\hat{P}^i\frac{1}{h_i}\frac{\partial \alpha}{\partial x^i} - \sum_{i,j}\hat{T}^{ij}\sigma_{ij}, \tag{57}$$

$$\hat{E}^i = -\sum_{j,k}\epsilon_{ijk}\hat{v}^j\hat{B}^k, \tag{58}$$

$$\frac{\partial \hat{B}_i}{\partial t} = \frac{-h_i}{h_1h_2h_3}\sum_{j,k}\epsilon^{ijk}\frac{\partial}{\partial x^j}\left[\alpha h_k(\hat{E}_k - \sum_{l,m}\epsilon^{klm}c\beta^l\hat{B}_m)\right], \tag{59}$$

$$\sum_i \frac{1}{h_1h_2h_3}\frac{\partial}{\partial x^i}\left(\frac{h_1h_2h_3}{h_i}\hat{B}_i\right) = 0, \tag{60}$$

$$\rho_{\rm e} = \sum_i \frac{1}{c^2}\frac{\alpha}{h_1h_2h_3}\frac{\partial}{\partial x^i}\left(\frac{h_1h_2h_3}{h_i}\hat{E}_i\right), \tag{61}$$

$$\hat{J}^i + \rho_{\rm e}c\beta^i + \frac{1}{c^2}\frac{\partial \hat{E}_i}{\partial t} = + \sum_{j,k}\frac{h_i}{h_1h_2h_3}\epsilon^{ijk}\frac{\partial}{\partial x^j}\left[\alpha h_k\left(\hat{B}_k + \sum_{l,m}\epsilon_{klm}\beta^l\frac{\hat{E}_k}{c}\right)\right], \tag{62}$$

where $f^i_{\rm curv} \equiv \sum_j (G_{ij}\hat{T}^{ij} - G_{ji}\hat{T}^{jj})$, $G_{ij} \equiv -\frac{1}{h_ih_j}\frac{\partial h_i}{\partial x^j}$, and $\sigma_{ij} \equiv \frac{h_i}{h_j}\frac{\partial \omega_i}{\partial x^j}$. This form of the equation is called *3+1 form*, because the derivatives with respect to time and space are separated completely (Thorne, Price, & Macdonald 1986).

Through this is paper, we normalize the magnetic field $\mathbf{B}$ and electric field $\mathbf{E}$ so that $B^2/2$ and $E^2/2c^2$ present the magnetic and electric field energy density, respectively. We also normalize the electric charge density $\rho_{\rm e}$ and the electric current density $\mathbf{J}$ as the Lorentz force density is given by $\rho_{\rm e}\mathbf{E} + \mathbf{J}\times\mathbf{B}$. For example, the normalized variables used here are related with the variables in MKSA unit system (SI unit system) as follows:

$$\mathbf{B} = \frac{\mathbf{B}^*}{\sqrt{\mu_0}}, \qquad \mathbf{E} = \frac{\mathbf{E}^*}{\sqrt{\mu_0}}, \tag{63}$$

$$\rho_{\rm e} = \sqrt{\mu_0}\rho^*_{\rm e}, \qquad \mathbf{J} = \sqrt{\mu_0}\mathbf{J}^*, \tag{64}$$

where a quantity with an asterisk is in the MKSA unit system (SI unit system).

(d) Vector Form of GRMHD Equations

We introduce the derivatives in the three-vector and scalar fields measured by FIDO. Here $\hat{\mathbf{a}}$ and $\hat{\mathbf{b}}$ are arbitrary three-vector fields and $\hat{\phi}$ is arbitrary scalar field measured by FIDO. We list up the definitions as follows,

$$\hat{\nabla}\cdot\hat{\mathbf{a}} = \sum_i \frac{1}{h_1h_2h_3}\frac{\partial}{\partial x^i}\left(\frac{h_1h_2h_3}{h_i}\hat{a}^i\right), \tag{65}$$

$$(\hat{\nabla}\hat{\phi})_i = \frac{1}{h_i}\frac{\partial \hat{\phi}}{\partial x^i}, \tag{66}$$

$$(\hat{\nabla}\times\hat{\mathbf{a}})_i = \sum_{j,k}\frac{h_i}{h_1h_2h_3}\epsilon_{ijk}\frac{\partial}{\partial x^j}(h_k\hat{a}^k), \tag{67}$$

$$[(\hat{\mathbf{b}}\cdot\hat{\nabla})\hat{\mathbf{a}}]_i = \sum_j\left[\frac{\hat{b}^j}{h_j}\frac{\partial \hat{a}^i}{\partial x^j} - G_{ij}\hat{a}^j\hat{b}^i + G_{ji}\hat{a}^j\hat{b}^j\right]. \tag{68}$$

Using these definitions, all formulae of the vector analysis can be used without modification except for the following equation,

$$(\hat{\nabla}\times\hat{\mathbf{a}})\times\hat{\mathbf{b}} = (\hat{\mathbf{b}}\cdot\hat{\nabla})\hat{\mathbf{a}} - (\hat{\nabla}\hat{\mathbf{a}})\cdot\hat{\mathbf{b}} + [\hat{\mathbf{a}},\hat{\mathbf{b}}], \tag{69}$$

where $[(\hat{\nabla}\hat{\mathbf{a}})\cdot\hat{\mathbf{b}}]_i \equiv \sum_j \frac{1}{h_i}\frac{\partial \hat{a}^j}{\partial x^i}\hat{b}^j$ and $[\hat{\mathbf{a}},\hat{\mathbf{b}}]_i \equiv \sum_j G_{ij}(\hat{a}^j\hat{b}^i - \hat{a}^i\hat{b}^j)$. It is also noted with respect to a formula,

$$\hat{\nabla}\times(\hat{\mathbf{a}}\times\hat{\mathbf{b}}) = (\hat{\nabla}\cdot\hat{\mathbf{b}})\hat{\mathbf{a}} + (\hat{\mathbf{b}}\cdot\hat{\nabla})\hat{\mathbf{a}} - (\hat{\nabla}\cdot\hat{\mathbf{a}})\hat{\mathbf{b}} - (\hat{\mathbf{a}}\cdot\hat{\nabla})\hat{\mathbf{b}}, \tag{70}$$

we often use more useful following equation of the components,

$$[\hat{\nabla}\times(\hat{\mathbf{a}}\times\hat{\mathbf{b}})]_i = (\hat{\nabla}\cdot\hat{\mathbf{b}})\hat{a}^i - (\hat{\nabla}\cdot\hat{\mathbf{a}})\hat{b}^i + \sum_j\frac{h_i}{h_j}\left[\hat{b}^j\frac{\partial}{\partial x^j}\left(\frac{\hat{a}^i}{h_i}\right) - \hat{a}^j\frac{\partial}{\partial x^j}\left(\frac{\hat{b}^i}{h_i}\right)\right]. \tag{71}$$

Using the derivatives of the three-vector and scalar fields, we write the equations of GRMHD with components (55)-(62) in the vector form,

$$\frac{\partial D}{\partial t} = -\hat{\nabla}\cdot[\alpha D(\hat{\mathbf{v}} + c\underline{\beta})], \tag{72}$$

$$\frac{\partial \hat{\mathbf{P}}}{\partial t} = -\hat{\nabla}\cdot[\alpha(\hat{\mathbf{T}} + c\underline{\beta}\hat{\mathbf{P}})] - (\epsilon + Dc^2)\hat{\nabla}\alpha + \alpha\mathbf{f}_{\rm curv} - \hat{\mathbf{P}}\cdot\sigma, \tag{73}$$

$$\frac{\partial \epsilon}{\partial t} = -\hat{\nabla}\cdot[\alpha(c^2\hat{\mathbf{P}} - Dc^2\hat{\mathbf{v}} + \epsilon c\underline{\beta})] - (\hat{\nabla}\alpha)\cdot c^2\hat{\mathbf{P}} - \hat{T} : \sigma, \tag{74}$$

$$\frac{\partial \hat{\mathbf{B}}}{\partial t} = -\hat{\nabla}\times[\alpha(\hat{\mathbf{E}} - c\underline{\beta}\times\hat{\mathbf{B}})], \tag{75}$$

$$\hat{\mathbf{J}} + \hat{\rho}_{\rm e}c\underline{\beta} + \frac{1}{c^2}\frac{\partial \hat{\mathbf{E}}}{\partial t} = \hat{\nabla}\times[\alpha(\hat{\mathbf{B}} + \frac{1}{c}\underline{\beta}\times\hat{\mathbf{E}})], \tag{76}$$

$$\hat{\nabla}\cdot\hat{\mathbf{B}} = 0, \tag{77}$$

$$\hat{\rho}_{\rm e} = \frac{\alpha}{c^2}\hat{\nabla}\cdot\hat{\mathbf{E}}, \tag{78}$$

$$\hat{\mathbf{E}} + \hat{\mathbf{v}}\times\hat{\mathbf{B}} = \mathbf{0}, \tag{79}$$

where $\underline{\beta}$ is three-vector with the components β_i, $\underline{\beta} = (\beta_1, \beta_2, \beta_3)$.

(e) Comparison of Conservative and Advective Form of Relativistic MHD Equations

We compare the usage of conservative and advective form. To develop the GRMHD code from the special relativistic MHD code, we just add some terms and factors with respect to the metric (h_i, ω_i, and σ_{ij}) in the time-boost part. It is straightforward and not so difficult. The difficulty in the development of relativistic MHD code is in that of the special relativistic MHD code. Therefore, here we consider the special relativistic MHD. The conservative form of special relativistic MHD is as follows,

$$\frac{\partial D}{\partial t} = -\nabla\cdot(D\mathbf{v}), \tag{80}$$

$$\frac{\partial \mathbf{P}}{\partial t} = -\nabla\cdot\left[\left(p + \frac{B^2}{2} + \frac{E^2}{2c^2}\right)\mathsf{I} + \frac{h}{c^2}\gamma^2\mathbf{v}\mathbf{v} - \mathbf{B}\mathbf{B} - \frac{\mathbf{E}\mathbf{E}}{c^2}\right], \tag{81}$$

$$\frac{\partial \epsilon}{\partial t} = -\nabla\cdot[c^2\mathbf{P} - Dc^2\mathbf{v}], \tag{82}$$

$$\frac{\partial \mathbf{B}}{\partial t} = -\nabla\times\mathbf{E}, \tag{83}$$

$$\mathbf{E} = -\mathbf{v}\times\mathbf{B}, \tag{84}$$

$$\nabla\cdot\mathbf{B} = 0, \tag{85}$$

$$\rho_{\rm e} = \frac{1}{c^2}\nabla\cdot\mathbf{E}, \tag{86}$$

$$\mathbf{J} + \frac{1}{c^2}\frac{\partial \mathbf{E}}{\partial t} = \nabla\times\mathbf{B}, \tag{87}$$

where I is the (3×3) unit tensor.

The equations with respect to the electromagnetic field (83) - (87) are common in the both forms. The different equations in advective form corresponding to the equations (80) - (82) are

$$\frac{dD}{dt} = -D\nabla\cdot\mathbf{v}, \tag{88}$$

$$\gamma\rho\frac{d}{dt}\left(\frac{h\gamma\mathbf{v}}{\rho c^2}\right) = -\nabla p + \rho_{\rm e}\mathbf{E} + \mathbf{J}\times\mathbf{B}, \tag{89}$$

$$\frac{d}{dt}(\gamma^\Gamma p) = -\Gamma\gamma^\Gamma p(\nabla\cdot\mathbf{v}), \tag{90}$$

where $d/dt \equiv \partial/\partial t + (\mathbf{v}\cdot\nabla)$ is the convective derivative. It is easier to get primitive variables from the variables boosted by the advective form than that by conservative form. However, in the advective form, we should calculate the current density $\mathbf{J}$. It is not so easy because we have to treat the displacement current $c^{-2}\partial\mathbf{E}/\partial t$ is the Ampere law (87). Therefore, we use the convective form for relativistic MHD simulations.

III. NUMERICAL METHOD

We employ the *simplified total variation diminishing* (TVD) method for GRMHD simulations (see Koide et al. 1999, Appendix D), which was developed by Davis (1984) for violent phenomena such as shocks. This method is similar to Lax-Wendroff's method with the addition of a diffusion term formally. In order to integrate the time-dependent conservation laws, we need only the maximum speed of waves and not each eigenvector or eigenvalue of the Jacobian of the linearized GRMHD equations.

With the simplified TVD method, we obtain only the quantities D, $\hat{\mathbf{P}}$, ϵ, and $\hat{\mathbf{B}}$ directly at each step from the difference equations. In the next step, we must calculate the primitive variables $\hat{\mathbf{v}}$ and p from D, $\hat{\mathbf{P}}$, ϵ, and $\hat{\mathbf{B}}$ from equations (44),(45),(46), and (48). To do this, we solve two nonlinear, simultaneous algebraic equations with unknown variables $x \equiv \hat{\gamma} - 1$ and $y \equiv \hat{\gamma}(\hat{\mathbf{v}}\cdot\hat{\mathbf{B}})/c^2$,

$$x(x+2)\left[\Gamma R x^2 + (2\Gamma R - d)x + \Gamma R - d + u + \frac{\Gamma}{2}y^2\right]^2$$

$$= (\Gamma x^2 + 2\Gamma x + 1)^2[f^2(x+1)^2 + 2\sigma y + 2\sigma x y + b^2 y^2], \tag{91}$$

$$[\Gamma(R - b^2)x^2 + (2\Gamma R - 2\Gamma b^2 - d)x + \Gamma R - d + u - b^2 + \frac{\Gamma}{2}y^2]y$$

$$= \sigma(x+1)(\Gamma x^2 + 2\Gamma x + 1), \tag{92}$$

where $R = D + \hat{\epsilon}/c^2$, $d = (\Gamma - 1)D$, $u = (1 - \Gamma/2)\hat{B}^2/c^2$, $f = \hat{P}/c$, $b = \hat{B}/c$, and $\sigma = \hat{\mathbf{B}}\cdot\hat{\mathbf{P}}/c^2$. It is noted that in the absence of the magnetic field equation (91) becomes the equation in the relativistic hydrodynamic case, as derived by Duncan & Hughes (1994), and equation (92)

becomes a trivial equation. The equations are solved at each cell using a 2-variable Newton-Raphson iteration method. We then easily calculate p and $\hat{\mathbf{v}}$ using x, y, D, $\hat{\mathbf{P}}$, ϵ, and $\hat{\mathbf{B}}$. This method is identical to that in the special relativistic case (Koide, Nishikawa, & Mutel 1996; Koide 1997).

IV. FORMULAE FOR TEST PROBLEMS

We summarize the useful formulae for the test problems and check of the GRMHD code.

(a) Motion of Particle around Kerr Black Hole

We consider a neutral particle with the proper mass m moving around the Kerr black hole. If no external force acts on the particle, there are two kinds of conservation quantities. One is energy-at-infinity,

$$E^{\infty} = \alpha mc^2\gamma + \omega_3 h_3 m\gamma\hat{v}^{\phi}, \tag{93}$$

and the other is angular momentum

$$L = h_3 m\gamma\hat{v}^{\phi}. \tag{94}$$

The energy-at-infinity is also written as

$$E^{\infty} = \alpha\hat{E} + \omega_3 L, \tag{95}$$

where

$$\hat{E} = mc^2\gamma \tag{96}$$

is the total energy of the particle observed by FIDO. Let us consider the particle motion in the equatorial plane. In the case, the co-latitude component of the velocity is zero ($\hat{v}_\theta = 0$) and the Lorentz factor of the particle is written by

$$\gamma = \sqrt{\frac{1 + \left(\frac{L}{mch_3}\right)^2}{1 - \left(\frac{\hat{v}_r}{c}\right)^2}}. \tag{97}$$

Then the energy-at-infinity is

$$\frac{E^{\infty}}{mc^2} = \alpha\sqrt{\frac{1 + \left(\frac{L}{mch_3}\right)^2}{1 - \left(\frac{\hat{v}_r}{c}\right)^2}} + \omega_3\frac{L}{mc^2}. \tag{98}$$

This satisfies the following inequality,

$$\frac{E^{\infty}}{mc^2} \geq \alpha\sqrt{1 + \left(\frac{L}{mch_3}\right)^2} + \omega_3\frac{L}{mc^2} \equiv \Phi(r), \tag{99}$$

where the equal stands only for $\hat{v}^r = 0$. The function of r, $\Phi(r)$ is the effective gravitational potential.

On the case with the zero angular momentum, $L = 0$, the equation (98) yields

$$\frac{E^{\infty}}{mc^2} = \frac{\alpha}{\sqrt{1 - \left(\frac{\hat{v}^r}{c}\right)^2}} = \alpha\gamma = (\text{const}). \tag{100}$$

This equation provide free fall velocity of the particle into the Kerr black hole. In the Schwarzschild black hole case, it gives

$$\hat{v}^r = -\alpha\sqrt{\frac{r_{\rm S}}{r}}, \tag{101}$$

when $E^{\infty} = mc^2$.

Motion of a particle in the circular orbit around the central object is called *Kepler rotation*. Here we assume the orbit is in the equatorial plane. The motion is realized when $\partial\Phi/\partial r = 0$. The azimuthal component of the velocity is given by

$$\tilde{v}^{\phi}_{\rm K} = c\frac{A}{\sqrt{\Delta}(r^3 - r_{\rm g}^3 a^2)}\left[\pm\sqrt{\frac{r_{\rm g}}{r}} - \frac{ar_{\rm g}^2}{r^2}\right], \tag{102}$$

where the positive (negative) sign corresponds to the case in which the particle rotates in the same (opposite) direction as the black hole rotation. This velocity is called *Kepler velocity*. We find that the velocity of the opposite rotation case is larger than that of the corotation case. It is noted that $\tilde{v}^{\phi}_{\rm K}$ is the velocity observed by LOLA frame. The velocity by FIDO frame is given by $\hat{v}^{\phi}_{\rm K} = \tilde{v}^{\phi}_{\rm K} - c\beta^{\phi}$. On the case of Schwarzschild black hole ($a = 0$), the velocity is $\hat{v}^{\phi}_{\rm K} = \pm c/\sqrt{2(r/r_{\rm S} - 1)}$.

The orbit is unstable when $\partial\Phi/\partial r = 0$ and $\partial^2\Phi/\partial r^2 < 0$ or $\partial L_{\rm K}/\partial r < 0$, where $L_{\rm K}$ is the angular momentum of the particle in Kepler rotation, $L_{\rm K} = h_3 m\hat{\gamma}\hat{v}^{\phi}_{\rm K}$ and $\hat{\gamma}$ is Lorentz factor of the particle. The *last stable orbit* is determined by $\partial L_{\rm K}/\partial r = 0$. On the Schwarzschild black hole case ($a = 0$), the radius of the last stable orbit is $r = 3r_{\rm S}$. On the maximumly rotating black hole case ($a = 1$), the radius is $r = 4.5r_{\rm S}$ when the particle rotates in the opposite direction of the black hole rotation, while the corotating particle is always stable when the particle rotates in the same direction.

(b) Penrose Process

We present a brief review of the *Penrose process*. We consider the fission of a particle near the Kerr black hole. For simplicity, we assume the particles move only in the equatorial plane. When a particle '0' is injected into the region near black hole with the energy-at-infinity E^{∞}_0 and the angular momentum L_0 and the fission of the particle produces two particles "1" and "2" with the energy-at-infinity E^{∞}_1, E^{∞}_2 and the angular momentum L_1, L_2, respectively. The conservation laws of the energy and angular momentum are

$$E^{\infty}_0 = E^{\infty}_1 + E^{\infty}_2, \tag{103}$$

$$L_0 = L_1 + L_2. \tag{104}$$

If the particle "2" is recoiled by the fission strongly and has the significant negative angular momentum, the energy-at-infinity of the particle "2" becomes negative, E^{∞}_2. Here we assume ω_3 is positive. In such

case, the energy-at-infinity of the particle "1" , E_1^∞ is greater than that of the injected particle "0", E_0^∞, because of the conservation of the total energy-at-infinity (103). On the other hand, the particle "2" is swallowed by the black hole and the rotation energy of the black hole decreases. This extraction process of the black hole rotational energy is *Penrose process*. The condition for the negative energy-at-infinity is derived from equations (103) and (104). When the relative velocity of the two particles "1" and "2" is Δv, the condition is written by

$$1 < \frac{\Delta v}{c}\frac{\beta^\phi + v_0^\phi/c}{1+\beta^\phi v_0^\phi/c}, \tag{105}$$

where we consider only azimuthal fission. Because outside of the ergosphere, $|\beta^\phi| < 1$, the right hand side of the inequality (105) is less than unity. In the ergosphere, $\beta^\phi > 1$ and the inequality is possible. When $\beta^\phi > 1$, we get

$$1 < \frac{\Delta v}{c}\frac{\beta^\phi + v_0^\phi/c}{1+\beta^\phi v_0^\phi/c} < \frac{\Delta v}{c}\beta^\phi. \tag{106}$$

Even if the case with $\beta^\phi = 0.5$ (which correspond to deep area in the ergosphere and near the event horizon around the very rapidly rotating black hole), it indicates $\Delta v > 0.5c$. This means the Penrose process demands the relativistic fission.

(c) Wald Solution

We show steady uniform magnetic field around a Kerr black hole in the vacuum, which is called *Wald solution* (Wald 1974). The vector potential is

$$A_\mu = \frac{B_0}{2}(g_{\mu 3} + 2ar_{\rm g}g_{\mu 0}), \tag{107}$$

where B_0 is constant indicating the magnetic field strength. Here we use the Boyer-Lindquist coordinates $(x^0, x^1, x^2, x^3) = (ct, r, \theta, \phi)$. This yields

$$\hat{B}_r = B_0\frac{\cos\theta}{\sqrt{A}}\left[\Delta + \frac{2r_{\rm g}r(r^4 - (ar_{\rm g})^4)}{\Sigma^2}\right], \tag{108}$$

$$\hat{B}_\theta = -\frac{B_0}{h_r}\sqrt{\frac{\Sigma}{A}}\sin\theta[r - r_{\rm g} + \frac{r_{\rm g}}{\Sigma^2}\{(r^2+(ar_{\rm g})^2)\Sigma + 2(ar_{\rm g})^2\cos^2\theta(r^2-(ar_{\rm g})^2)\}]. \tag{109}$$

(d) Frame-dragging Dynamo

The shear of the plasma flow observed by the Boyer-Lindquist frame due to the frame dragging effect of the rotating black hole causes the amplification of the magnetic field. This effect is called a *frame-dragging dynamo* (Yokosawa 1993; Meier 1999). With the assumption that the azimuthal velocity component is zero, general relativistic Faraday law of induction (59) and ideal MHD condition (58) yield,

$$\frac{\partial \hat{B}_\phi}{\partial t} = f_1\hat{B}_r + f_2\hat{B}_\theta, \tag{110}$$

where

$$f_1 = c\frac{h_3}{h_1}\frac{\partial}{\partial r}\left(\frac{\omega_3}{c}\right), \tag{111}$$

$$f_2 = c\frac{h_3}{h_2}\frac{\partial}{\partial \theta}\left(\frac{\omega_3}{c}\right). \tag{112}$$

It is noted that f_2 is one order smaller than f_1 when $a \sim 1$. The ridge of the f_1 profile is located near the spherical surface, $r = r_{\rm S}$ and the magnetic pressure has a maximal near the surface. This phenomena is useful for test problem of the GRMHD code.

The non-zero azimuthal component of the magnetic field corresponds to the twist of the magnetic field lines. This twist of the magnetic field line propagates outward along the magnetic field lines as torsional Alfvén wave. Alfvén velocity in the uniform plasma with the proper mass density ρ_0 and pressure p_0 and the uniform magnetic field $\mathbf{B_0}$ without the gravity is

$$v_{\rm A} = c\frac{B_0}{\sqrt{\rho_0 c^2 + \Gamma p_0/(\Gamma-1) + B_0^2}}. \tag{113}$$

The fast velocity is

$$v_{\rm f} = c\sqrt{\frac{B_0^2 + \Gamma p_0}{\rho_0 c^2 + \Gamma p_0/(\Gamma-1) + B_0^2}}. \tag{114}$$

When we put $B_0 = 0$ in equation (114), it yields the relativistic sound speed,

$$v_{\rm s} = c\sqrt{\frac{\Gamma p_0}{\rho_0 c^2 + \Gamma p_0/(\Gamma-1)}}. \tag{115}$$

(e) Transport Equations

First, we present conservation equations of energy and angular momentum around Kerr black hole. The Killing vectors for Kerr geometry are $\chi^\nu = (-1,0,0,0)$ and $\eta^\nu = (0,0,0,-1)$. In general, any Killing vector ξ^ν presents conservation laws,

$$\frac{1}{\sqrt{-||g||}}\frac{\partial}{\partial x^\mu}(\sqrt{-||g||}T^{\mu\nu}\xi_\nu) = 0. \tag{116}$$

Using $||g|| = -(\alpha h_1 h_2 h_3)^2$, it becomes

$$\frac{\partial}{\partial t}(\alpha T^{0\nu}\xi_\nu) = -\frac{1}{h_1h_2h_3}\sum_i \frac{\partial}{\partial x^i}(\alpha h_1h_2h_3 cT^{i\nu}\xi_\nu). \tag{117}$$

When we use the Killing vector χ^ν, we get the following conservation law of energy,

$$\frac{\partial e^\infty}{\partial t} = -\hat{\nabla}\cdot(\alpha\mathbf{S}), \tag{118}$$

where $e^\infty \equiv \alpha T^{0\nu}\xi_\nu$ is called *energy-at-infinity* density and $S^i \equiv ch_i T^{i\nu}\xi_\nu$ is energy flux density. Here we also write these quantities as

$$e^\infty = \alpha(\epsilon + Dc^2) + \sum_i \omega_i h_i \hat{P}^i, \tag{119}$$

$$S^i = \alpha c^2 \hat{P}^i + e^\infty c\beta^i + \sum_j \alpha c \beta^j \hat{T}^{ij}. \tag{120}$$

The quantities can be divided to components as follows,

$$e^\infty = e^\infty_{\rm kin} + e^\infty_{\rm EM}, \tag{121}$$

$$S^i = S^i_{\rm kin} + S^i_{\rm EM}, \tag{122}$$

where

$$e^\infty_{\rm kin} = \alpha(h\gamma^2 - p) + \sum_i \omega_i h_i \frac{h}{c^2}\gamma^2 \hat{v}^i, \tag{123}$$

$$e^\infty_{\rm EM} = \alpha\left(\frac{\hat{B}^2}{2} + \frac{\hat{E}^2}{2c^2}\right) + \sum_i \omega_i h_i \frac{1}{c^2}(\hat{\mathbf{E}}\times\hat{\mathbf{B}})_i, \tag{124}$$

$$S^i_{\rm kin} = \alpha h\gamma^2 \left(1 + \sum_j \frac{c\beta^j \hat{v}^j}{c^2}\right)(\hat{v}^i + c\beta^i), \tag{125}$$

$$S^i_{\rm EM} = \alpha\left[(\hat{\mathbf{E}} - c\underline{\beta}\times\hat{\mathbf{B}})\times\left(\hat{\mathbf{B}} + c\underline{\beta}\times\frac{\hat{\mathbf{E}}}{c^2}\right)\right]^i, \tag{126}$$

where the subscript 'kin' and 'EM' indicate the kinetic and the electromagnetic components, respectively. With respect to the Killing vector η^ν, we have the following conservation equation of angular momentum.

$$\frac{\partial l}{\partial t} = -\hat{\nabla}\cdot(\alpha\mathbf{M}), \tag{127}$$

where $l \equiv \alpha T^{0\nu}\eta_\nu/c$ and $M^i \equiv h_i T^{i\nu}\eta_\nu$. Using the quantities measured by FIDO, we write

$$l = h_3 \hat{P}^3 \tag{128}$$

and

$$M^i = h_3(\hat{T}^{i3} + c\beta^i \hat{P}^3). \tag{129}$$

These variables are also divided into the kinetic and the electromagnetic components denoted by the suffix 'kin' and 'EM', respectively as follows,

$$l = l_{\rm kin} + l_{\rm EM}, \tag{130}$$

$$M^i = M^i_{\rm kin} + M^i_{\rm EM}, \tag{131}$$

where

$$l_{\rm kin} = h_3 \frac{h}{c^2}\gamma^2 \hat{v}^3, \tag{132}$$

$$l_{\rm EM} = \frac{h_3}{c^2}(\hat{\mathbf{E}}\times\hat{\mathbf{B}})_3, \tag{133}$$

$$M^i_{\rm kin} = h_3\left[p\delta^{i3} + \frac{h}{c^2}\gamma^2\hat{v}^i\hat{v}^3 + c\beta^i\frac{h}{c^2}\gamma^2\hat{v}^3\right], \tag{134}$$

$$M^i_{\rm EM} = h_3\left[\left(\frac{\hat{B}^2}{2} + \frac{\hat{E}^2}{2c^2}\right)\delta^{i3} - \hat{B}^i\hat{B}^3 - \frac{\hat{E}^i\hat{E}^3}{c^2} + \frac{c\beta^i}{c^2}(\hat{\mathbf{E}}\times\hat{\mathbf{B}})_3\right]. \tag{135}$$

We can see that the kinetic energy-at-infinity and angular momentum densities (123) and (132) are similar to those of one particle (93) and (94), respectively. When we notice $\hat{B}^2/2 + \hat{E}^2/2c^2$ and $\hat{\mathbf{E}}\times\hat{\mathbf{B}}/c^2$ correspond to effective electromagnetic mass density and momentum density in ZAMO frame, we find the similarity between the electromagnetic energy-at-infinity, angular momentum (124), (133) and those of one particle (93) and (94).

Next we present the transport equations of electromagnetic energy and momentum around Kerr black hole. The general relativistic Maxwell equations (75)-(78) yields,

$$\frac{\partial e^\infty_{\rm EM}}{\partial t} = -\hat{\nabla}\cdot(\alpha\mathbf{S}_{\rm EM}) - \alpha(\hat{\mathbf{v}} + c\underline{\beta})\cdot\mathbf{f}_{\rm L}, \tag{136}$$

$$\frac{\partial l_{\rm EM}}{\partial t} = -\hat{\nabla}\cdot(\alpha\mathbf{M}_{\rm EM}) - h_3 f^3_{\rm L}, \tag{137}$$

where $\mathbf{f}_{\rm L} = \rho_{\rm e}\hat{\mathbf{E}} + \hat{\mathbf{J}}\times\hat{\mathbf{B}}$ is the Lorentz force density. Subtracting the both hands of the electromagnetic transport equations (136), (137) from the conservation equations (118), (127), respectively, we found the kinetic transport equations of energy and angular momentum,

$$\frac{\partial e^\infty_{\rm kin}}{\partial t} = -\hat{\nabla}\cdot(\alpha\mathbf{S}_{\rm kin}) + \alpha(\hat{\mathbf{v}} + c\underline{\beta})\cdot\mathbf{f}_{\rm L}, \tag{138}$$

$$\frac{\partial l_{\rm kin}}{\partial t} = -\hat{\nabla}\cdot(\alpha\mathbf{M}_{\rm kin}) + h_3 f^3_{\rm L}. \tag{139}$$

When we write the suffix 'kin' and 'EM' by '+' and '-', respectively, the transport equation of energy and angular momentum are summarized as

$$\frac{\partial e^\infty_\pm}{\partial t} = -\hat{\nabla}\cdot(\alpha\mathbf{S}_\pm) \pm \alpha(\hat{\mathbf{v}} + c\underline{\beta})\cdot\mathbf{f}_{\rm L}, \tag{140}$$

$$\frac{\partial l_\pm}{\partial t} = -\hat{\nabla}\cdot(\alpha\mathbf{M}_\pm) \pm h_3 f^3_{\rm L}, \tag{141}$$

where the double signs are in same order.

V. A GRMHD SIMULATION OF JET FORMATION

We show a GRMHD simulation of jet formation from magnetized accretion disk around a rapidly rotating ($a = 0.95$) Kerr black hole (Koide et al. 2000). The simulations were performed for two cases in which the disk co-rotates and counter-rotates with respect to the

black hole rotation. Figures 1a-c illustrate the time evolution of the counter-rotating disk case and Fig. 1d the final state of the co-rotating case. These figures show the proper mass density (gray-scale), velocity (vectors), and magnetic field (solid lines) in $0 \le R \equiv r\sin\theta \le 7r_S$, $0 \le z \equiv r\cos\theta \le 7r_S$. The black region at the origin shows the inside of the black hole horizon, whose radius is $r_H = 0.656r_S$. The initial state in the simulation consists of a hot corona and a cold accretion disk around the black hole (Fig. 1a). In the corona, plasma is assumed to be in nearly stationary infall, with the specific enthalpy $h/\rho c^2 = 1 + \Gamma p/[(\Gamma-1)\rho c^2] = 1.3$, where specific heat ratio $\Gamma = 5/3$. The accretion disk is located at $|\cot\theta| \le 0.125$, $r \ge 3r_S$ and the initial velocity of the disk is assumed to be the Kepler velocity given by equation (102). Except for the disk rotation direction, we use the same initial conditions in both cases. The mass density of the disk is 100 times that of the corona at the inner edge of the disk. The mass density profile is given by that of a hydrostatic equilibrium corona with a scale height of $r_c \sim 3r_S$. The disk is in pressure balance with the corona, and the magnetic field lines are perpendicular to the accretion disk. We use the azimuthal component of the vector potential A_ϕ of the Wald solution (107) to set the magnetic field. Here the magnetic field strength is $B_0 = 0.3\sqrt{\rho_0 c^2}$, where ρ_0 is the initial corona density at $r = 3r_S$. The Alfvén velocity and plasma beta value at the disk ($r = 3.5r_S$) are $v_A = 0.03c$ and $\beta \equiv 2p/\hat{B}^2 \sim 3.4$, respectively.

Figure 1b shows the state at $t = 30\tau_S$, where τ_S is defined as $\tau_S \equiv r_S/c$. In the counter-rotating disk case, there is no stable circular orbit at $R \le 4.4r_S$, the disk falls into the black hole rapidly dragging the magnetic field lines. The disk enters the ergosphere and then crosses the horizon, as shown by the crowded magnetic field lines near $r = 0.75r_S$ (Fig. 1c). The jet is ejected almost along the magnetic field lines. Its maximum total and poloidal velocities are the same, $\hat{v} = \hat{v}_p = 0.44c$ at $R = 3.2r_S$, $z = 1.6r_S$. Inside the ergosphere, the velocity of frame dragging exceeds the speed of light ($c\beta^3 > c$), causing the disk to rotate in the *same* direction of the black hole rotation (relative to the Boyer-Lindquist frame), even though it was initially counter-rotating. The rapid, differential frame dragging enhances the azimuthal magnetic field, which is effect of the *frame-dragging dynamo*. This enhanced magnetic field pressure blows off the plasma upward and pinches it into a powerful collimated jet. In this case, the total energy-at-infinity density e^∞ is positive everywhere and the extraction of the net energy of the Kerr black hole is not realized. On the case with the very light disk, the negative energy-at-infinity state may be realized by strong magnetic field and the net energy extraction from black hole is possible like *Penrose process.*

Figure 1d shows a snapshot of the co-rotating disk case at $t = 47\tau_S$. The disk stops its infall near $R = 3r_S$ due to the centrifugal barrier with a shock at $r = 3.4r_S$. The high pressure behind the shock causes a gas pressure-driven jet with total and poloidal velocities of $\hat{v} = \hat{v}_p = 0.30c$ at $R = 3.4r_S$, $z = 2.4r_S$. The centrifugal barrier makes the disk take much long time to reach the ergosphere, which causes the difference between the co-rotating and counter-rotating disk cases.

VI. SUMMARY

In this paper, we present the whole basis of the method of numerical simulations for general relativistic MHD in Kerr space-time. We hope the readers use this paper as a guide book or a handbook to develop their own GRMHD code. We are planning to open one-dimensional version of our GRMHD code for public as a part of the ACT-JST project. Please visit the web site (http://www.astro.phys.s.chiba-u.ac.jp /netlab/).

ACKNOWLEDGEMENTS

We thank Mika Koide for her important comments for this study. We appreciate the support of the National Institute for Fusion Science and National Astronomical Observatory of Japan in the use of their super-computers and special devises for display. This work was supported in part by the Scientific Research Fund of the Japanese Ministry of Education, Culture, Sports, Science, and Technology and ACT-JST project of Japan Society of Technology Corporation.

REFERENCES

Biretta, J. A., Sparks, W. B., & Macchetto, F. 1999, ApJ, 520, 621

Davis, S. F. 1984, NASA Contractor Rep. 172373 (ICASE Rep. 84-20) (Washington: NASA)

Duncan, G. C. & Hughes, P. A. 1994, ApJ, 321. 334

Koide, S 1997, ApJ, 478, 66.

Koide, S., Meier, D. L., Shibata, K., & Kudoh, T. 2000, ApJ, 536, 668

Koide, S, Nishikawa, K.-I., & Mutel, R. L. 1996, ApJ, 463, L71

Koide, S., Shibata, K., & Kudoh, T. 1998, ApJ, 495, L63

——-. 1999, ibid., 522, 727

Kulkarni, S. R. 1999, Nature, 398, 389

Meier, D. 1999, ApJ, 522, 753

Mirabel, I. F. & Rodriguez, L. F. 1994, Nature, 374, 141

Pearson, T. J. & Zensus, J. A. 1987 in Superluminal Radio Sources, ed. J. A. Zensus & T. J. Pearson (London: Cambridge Univ.), p. 1

Thorne, K. S., Price, R. H., & Macdonald, D. A. 1986, *Membrane Paradigm* (New Haven: Yale Univ. Press)

Tingay, S. J. et al. 1995, Nature, 374, 141

Wald, R. M. 1974, Phys. Rev. D, 10, 1680

Weinberg, S. 1972, *Gravitation and Cosmology* (New York: Wiley.)

Yokosawa, M. 1993, PASJ, 45, 207

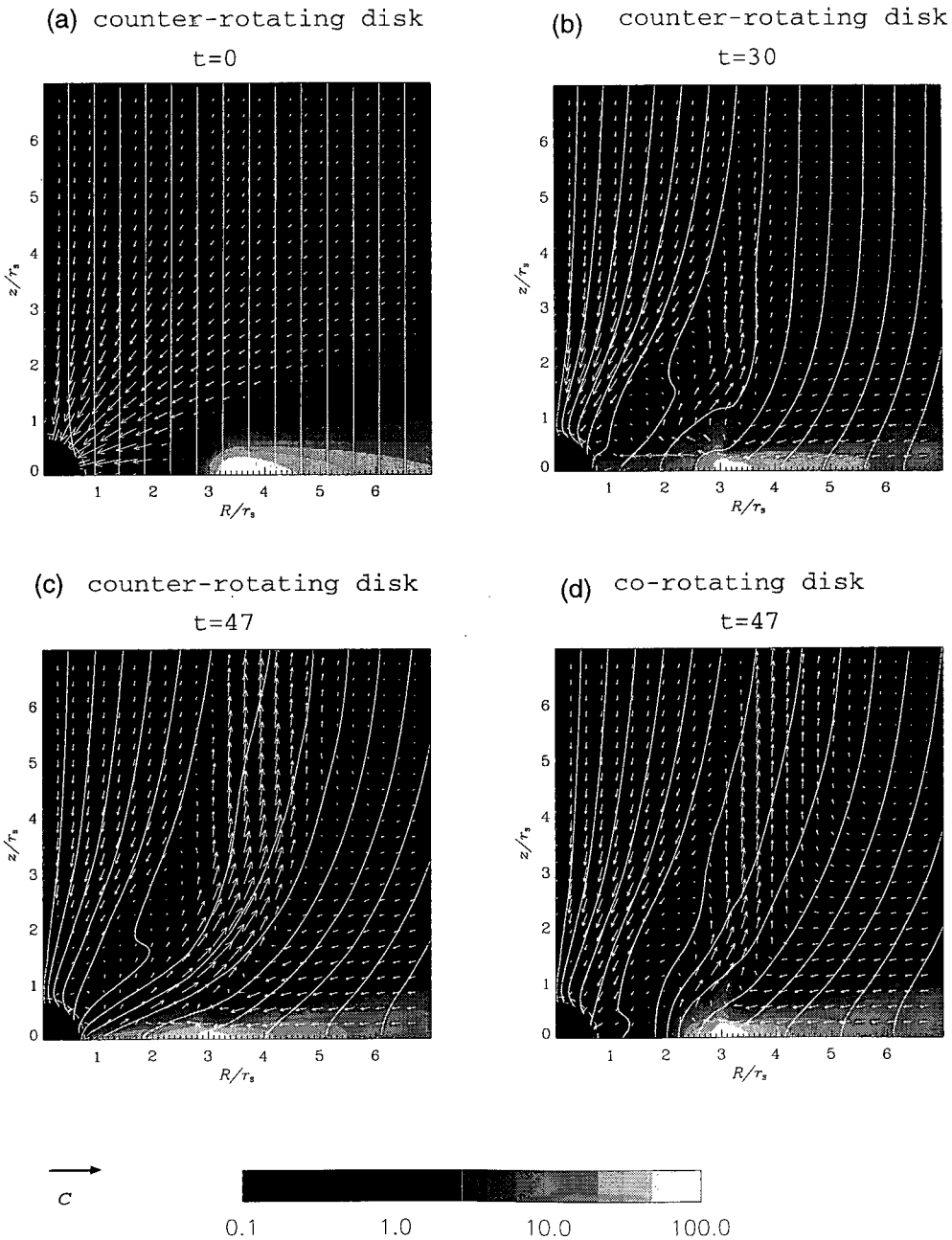

Fig. 1.— Time evolution of jet formation in the counter-rotating disk case and the final state of the co-rotating disk case. Gray-scale shows the logarithm of the proper mass density; vectors indicate velocity; solid lines show the poloidal magnetic field. The black fan-shaped region at the origin shows the horizon of the Kerr black hole ($a = 0.95$). The dashed line near the horizon is the inner boundary of the calculation region. At $t = 47\tau_S$, while the infall of the disk in the co-rotating disk stops (due to a centrifugal barrier), the unstable orbits of the counter-rotating disk plasma continue to spiral rapidly toward the black hole horizon. This difference causes the magnetohydrodynamic jet formation mechanisms in the two cases to differ drastically, resulting in a powerful jet emanating from deep within the ergosphere.